Cell Reports
Methods

Article

Optimization and validation of CAR transduction into human primary NK cells using CRISPR and AAV

Graphical abstract

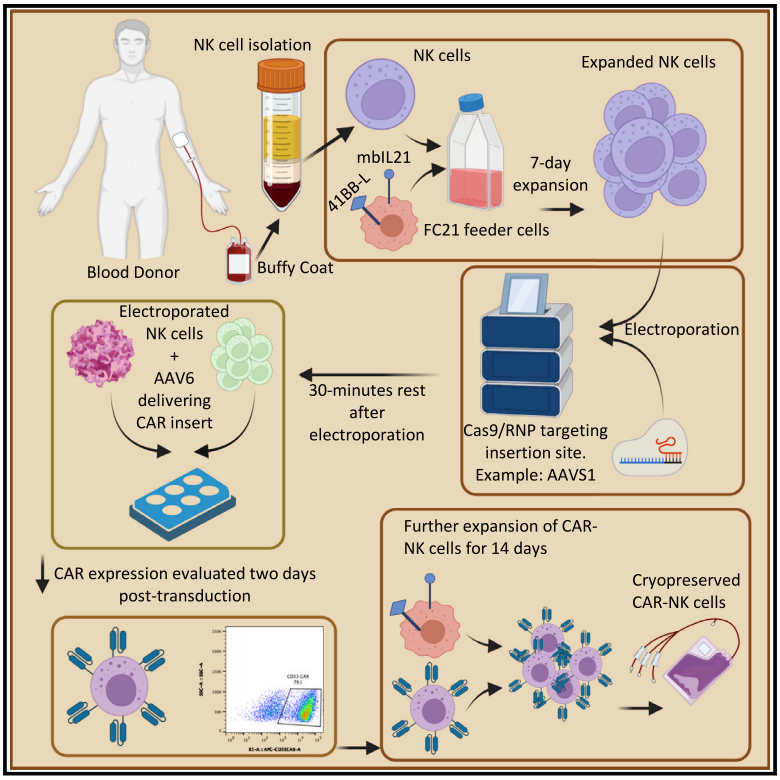

Highlights

- An efficient method for site-directed gene insertion in human primary NK cells
- Potential applications in cancer immunotherapy and for studying NK cell biology
- Genetically modified NK cells retain expression after expansion

Authors

Meisam Naeimi Kararoudi, Shibi Likhite, Ezgi Elmas, ..., Branden S. Moriarity, Kathrin Meyer, Dean A. Lee

Correspondence

dean.lee@nationwidechildrens.org

In brief

Naeimi Kararoudi et al. present an efficient method using CRISPR and AAV for site-directed gene knockin into human primary NK cells and show proof of concept by generating CD33-specific CAR-NK cells and demonstrating efficacy against AML. This approach has wide potential for therapeutic applications and the study of NK cell biology.

Naeimi Kararoudi et al., 2022, Cell Reports Methods 2, 100236
June 20, 2022
https://doi.org/10.1016/j.crmeth.2022.100236

CellPress

Cell Reports Methods

CellPress
OPEN ACCESS

Article

Optimization and validation of CAR transduction into human primary NK cells using CRISPR and AAV

Meisam Naeimi Kararoudi,[1,2] Shibi Likhite,[3] Ezgi Elmas,[1,6] Kenta Yamamoto,[4] Maura Schwartz,[3] Kinnari Sorathia,[1] Marcelo de Souza Fernandes Pereira,[1] Yasemin Sezgin,[1] Raymond D. Devine,[7] Justin M. Lyberger,[7] Gregory K. Behbehani,[7] Nitin Chakravarti,[5] Branden S. Moriarity,[4] Kathrin Meyer,[2,3] and Dean A. Lee[1,2,8,*]

[1]Center for Childhood Cancer and Blood Diseases, Abigail Wexner Research Institute at Nationwide Children's Hospital, Columbus, OH, USA
[2]Department of Pediatrics, The Ohio State University, Columbus, OH, USA
[3]Center for Gene Therapy, Abigail Wexner Research Institute at Nationwide Children's Hospital, Columbus, OH, USA
[4]Department of Pediatrics, University of Minnesota, Minneapolis, MN, USA
[5]Department of Medical Oncology, Thomas Jefferson University, Philadelphia, PA 19107, USA
[6]Molecular, Cellular and Developmental Biology Graduate Program, The Ohio State University, Columbus, OH, USA
[7]Department of Medicine, Division of Hematology, The Ohio State University Comprehensive Cancer Center, The Ohio State University, Columbus, OH 43210, USA
[8]Lead contact
*Correspondence: dean.lee@nationwidechildrens.org
https://doi.org/10.1016/j.crmeth.2022.100236

MOTIVATION NK cells have high potential as a source of immune effector cells (IECs) for the treatment of cancer and infectious diseases. Genetic modification of IECs with chimeric antigen receptors can improve their potency and efficacy, but methods for genetic engineering that work well for other IECs have proven difficult to adapt to human primary NK cells. Having previously shown that gene knockout could be accomplished with high efficiency in NK cells using electroporation of Cas9/RNP, we built on that approach to develop a robust method for site-directed gene insertion in human primary NK cells by combining Cas9/RNP electroporation and AAV transduction. This method allows investigators to generate precision-engineered NK cells with high transduction efficiency for cancer immunotherapy and basic biological studies.

SUMMARY

Human primary natural killer (NK) cells are being widely advanced for cancer immunotherapy. However, methods for gene editing of these cells have suffered low transduction rates, high cell death, and loss of transgene expression after expansion. Here, we developed a highly efficient method for site-specific gene insertion in NK cells using CRISPR (Cas9/RNP) and AAVs. We compared AAV vectors designed to mediate gene insertion by different DNA repair mechanisms, homology arm lengths, and virus concentrations. We then validated the method for site-directed gene insertion of CD33-specific CARs into primary human NK cells. CAR transduction was efficient, its expression remained stable after expansion, and it improved efficacy against AML targets.

INTRODUCTION

Human primary natural killer (NK) cells have been tested in numerous clinical trials demonstrating a high safety profile and evidence of clinical benefit for patients with cancer, which has been most widely applied to acute myelogenous leukemia (AML). Enhanced targeting of NK cells to AML through CD33 targeting has been shown with antibody Fc modifications (Romain et al., 2014; Mani et al., 2020) or fusion to alternative activation domains as bi- or tri-specific NK cell engagers (Gleason et al., 2014; Vallera et al., 2016). CD33 targeting by T cells has been enabled by CD33-targeting chimeric antigen receptors (CARs) (Dutour et al., 2012; Kim et al., 2018; Rotiroti et al., 2020), but clinical application has been hindered by concerns of long-term suppression of hematopoiesis with CAR-T persistence. Gene modification of NK cells to enable stable expression of a CAR can also improve their antitumor activity (Liu et al., 2020). However, gene modification of human peripheral-blood-derived NK cells (PB-NK) using viral or non-viral vectors has been challenging due to robust foreign DNA- and RNA-sensing mechanisms that limit the efficiency of these gene-delivery methods (Liu et al., 2020). Despite some improvements made in using lentiviral and retroviral transduction of human primary NK cells, the relative expression of CAR has been low. To overcome this limitation, mRNA-based gene delivery has been tested in PB-NK cells, but this only allows for

A

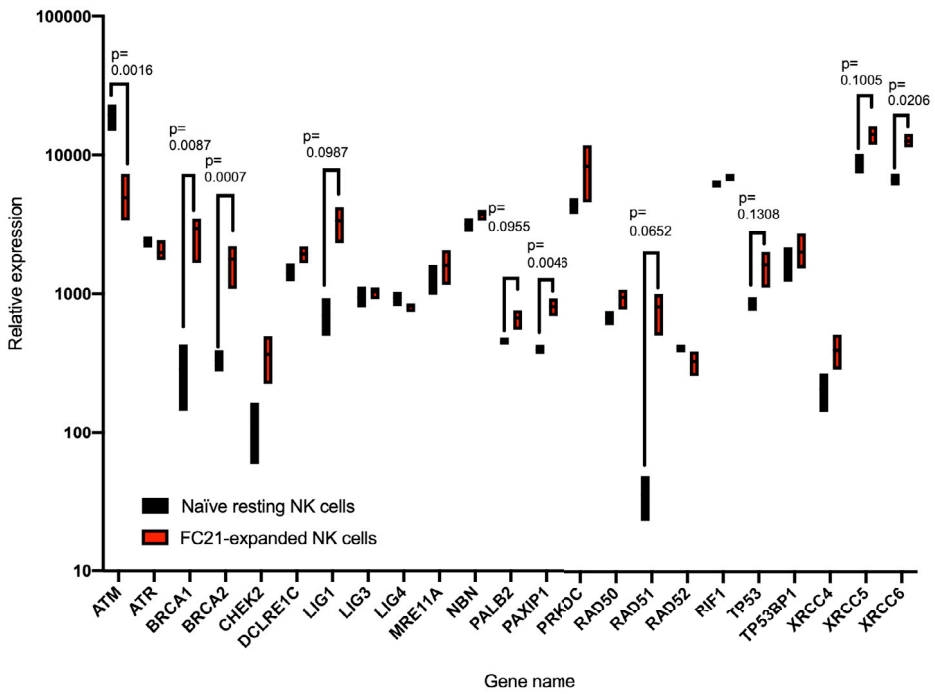

B

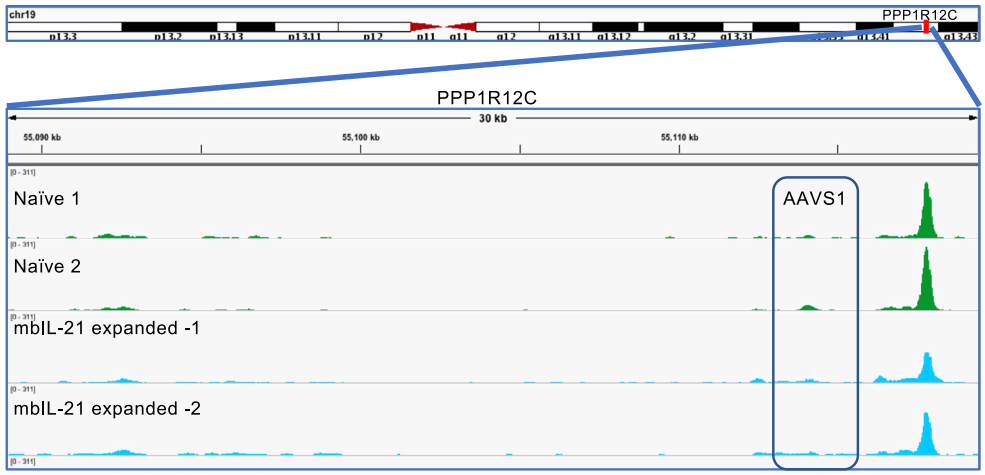

C

	Indel	Contribution	Sequence
	0	13%	CCCCTCCACCCCACAGTGGGGCCACTAGGGACAGGATTGGTGACAGAAAAGCCCCATCCTTAGGC **Reference Wildtype, crRNA target, PAM sequence**
Examples AAVS1^{KO}	-1	82.2%	CCCCTCCACCCCACAGTGGGGCCACTAGGGACAG- ATTGGTGACAGAAAAGCCCCATCCTTAGGC
	-4	1.1%	CCCCTCCACCCCACAGTGGGGCCACTAGGGA - - - - ATTGGTGACAGAAAAGCCCCATCCTTAGGC
	-21	0.7%	CCCCTCCACCCCAC- ATTGGTGACAGAAAAGCCCCATCCTTAGGC
	-9	0.6%	CCCCTCCACCCCACAGTGGGGCCAC - - - - - - - - - - - - GATTGGTGACAGAAAAGCCCCATCCTTAGGC

(legend on next page)

transient expression of transgenes (Naeimi Kararoudi et al., 2020b). We recently demonstrated highly efficient gene knockout in human primary NK cells by electroporating Cas9/ribonucleoprotein complexes (Cas9/RNP) (Pomeroy et al., 2020; Naeimi Kararoudi et al., 2018, 2020a). After Cas9 introduces a double-stranded break (DSB), two independent and innate DNA-repair mechanisms may be employed to repair the break: homologous directed recombination (HDR) through homology repair (HR) or non-homologous end joining (NHEJ). In the presence of a DNA template encoding a gene of interest, the exogenous gene can be integrated into the Cas9-targeting site using either of these repair mechanisms (Mali et al., 2013). There are several ways to provide the DNA template, including viral and non-viral methods. In non-viral approaches, the single-stranded or double-stranded DNA template is typically electroporated along with Cas9/RNP (Suzuki et al., 2016); however, it typically has a lower efficiency compared with viral transduction. For viral gene delivery, adeno-associated viruses (AAV), including AAV6, have been used safely as delivery vectors in clinical trials for primary immune cells, including T cells (Eyquem et al., 2017; Liu et al., 2019).

The Cas9/RNP-AAV approach has not been described in human primary NK cells. Here, we set to optimize this approach, wherein Cas9/RNP electroporation in primary human NK cells is followed by a DNA template encoding a transgene, with or without homology arms for Cas9 targeting site, delivered using single-stranded or self-complementary AAV6. Using this approach, we achieved simple yet highly efficient generation of stable transgene-modified human primary NK cells, including two CAR-NK cells that showed enhanced anti-AML activity. The gene-modified NK cells generated by the AAV-Cas9/RNP platform have utility for clinical applications such as CAR expression for antigen specific cancer immunotherapy and for studying NK cell biology.

RESULTS

Expansion of NK cells improves conditions for gene insertion

The DNA-modifying and -repairing enzymes required for NHEJ and HDR are different. NHEJ, which is essential for CRISPR-assisted insertion tagging (CRISPaint), utilizes KU80 (XRCC5), KU70 (XRCC6), DNA-PKcs (PRKDC), Artemis (DCLRE1C), and LigIV (LIG4), while ATM, MRN (MRE11, NBN, and RAD50), RAD51, BRCA1, and BRCA2 are important for mediating HDR (Chen et al., 2018; Schmid-Burgk et al., 2016). We previously showed that expansion of NK cells on feeder cells expressing membrane-bound interleukin-21 (IL-21; FC21) induces broad changes in gene expression (Denman et al., 2012). Therefore, we analyzed the expression level of genes involved in HDR and NHEJ in freshly isolated NK cells and after expansion to determine the time point at which these mechanisms would be most active. RNA sequencing (RNA-seq) showed that ATM expression decreased modestly, but all others were stable or increased, including large increases in BRCA1, BRCA2, RAD51, and LIG4 expression (Figure 1A). This suggests that conditions for both HDR- and NHEJ-directed gene insertion are active in expanded NK cells.

Targeting a genomic safe harbor for gene insertion

For gene insertion in NK cells, we chose the *adeno-associated virusAAV integration site 1* (*AAVS1*), which is an exemplary genomic safe-harbor locus within the *phosphatase 1 regulatory subunit 12C* (*PPP1R12C*) gene (Oceguera-Yanez et al., 2016; Mali et al., 2013). Chromatin accessibility of AAVS1 was similar in naive and day 7 expanded NK cells (n = 2) as determined by assay for transposase-accessible chromatin (ATAC)-seq (Figure 1B). Next, AAVS1 was targeted by electroporation of Cas9/RNP into day 7 expanded NK cells (Figure S1A) using previously optimized electroporation parameters that yield high NK cell editing efficiency (>80%) and viability (>90%) (Naeimi Kararoudi et al., 2018, 2020a). We did not observe any impact of AAVS1 deletion on NK cell cytotoxicity against AML (Figure S1B). After 48 h, the frequency of insertions and deletions (indels) in CRISPR-edited NK cells was determined using Inference of CRISPR Edits (ICE) using primers flanking the AAVS1 locus (Table S1) (Hsiau et al., 2018). The ICE results showed that up to 85% of CRISPR-modified NK cells had at least one indel at the AAVS1 Cas9-targeting site (Figure 1C).

Gene insertion in primary human NK cells using single-stranded AAV6 and Cas9/RNP

To compare the efficiency of gene insertion across DNA-repair mechanisms, we generated a parallel series of AAV6 vectors suitable for HDR-mediated gene insertion (Figure 2A) using both single-stranded and self-complementary designs with varying homology arm lengths and for NHEJ-mediated gene insertion with CRISPaint containing PAMgPAMg sequences (Figure 2B). To maximize HDR-mediated gene insertion, we identified homology arms (HAs) for the right and left sides of the flanking regions of the Cas9 targeting site in the AAVS1 locus, cloned these together with the mCherry gene into the backbone of a single-stranded AAV plasmid, and packaged this construct into the AAV6 viral capsid (Figure 2A) (Foust et al., 2013; Wang et al., 2016; Eyquem et al., 2017). It has been shown that the efficiency of recombination increases as the length of HAs increases (Ran et al., 2013; MacLeod et al., 2017; He et al., 2016; Song and Stieger, 2017; Li et al., 2014). Therefore, for the single-stranded AAV (ssAAV) backbone, we used the longest possible length of the left and right HAs for mCherry (800–1,000 bp of HAs; sequences provided in Table S3). The constructs also contained a splice acceptor downstream of the transgene to improve the transcription of the

Figure 1. Efficient CRISPR targeting of AAVS1 in FC21-expanded human primary NK cells

(A) Relative gene expression level of NHEJ- and HR-related genes in naive and FC21-expanded NK cells (n = 4).

(B) ATAC-seq data shows that AAVS1 has a similar chromatin accessibility between freshly isolated (naive) and FC21-expanded NK cells (n = 2).

(C) Efficiency of Cas9/RNP-mediated targeting of AAVS1 in NK cells. Reference genomic sequence for AAVS1 is shown in the top row, indicating the crRNA target sequence in red and the PAM sequence in blue. The mutated sequences that were identified, and their associated frequencies, are shown in the bottom rows. Data are shown as mean ± SD. Significant p values are indicated are from individual ratio paired t tests and are not adjusted for multiple comparisons.

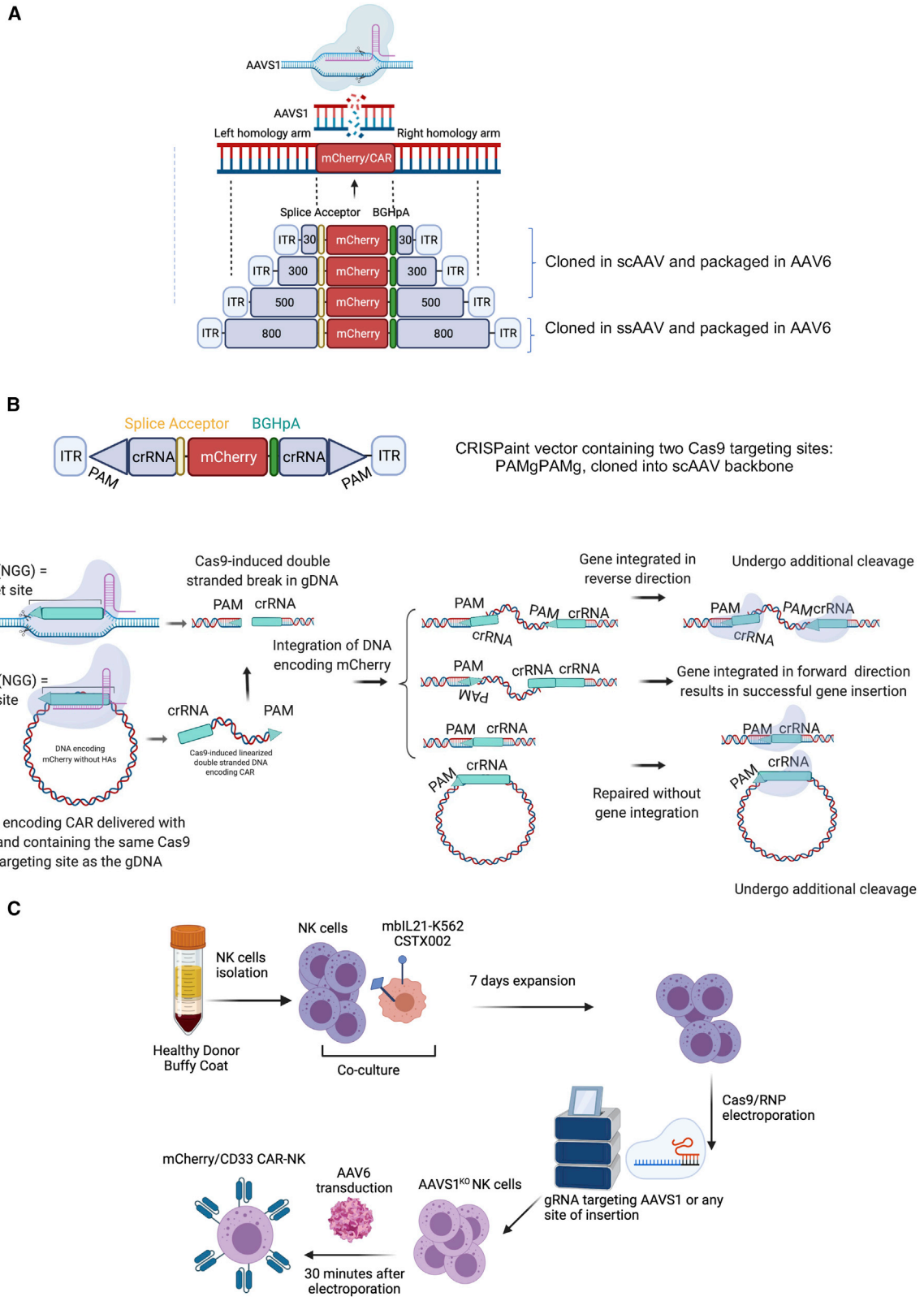

(legend on next page)

mCherry gene (Figure 2A). Electroporation of the NK cells with Cas9/RNP targeting AAVS1 followed 30 min later by AAV transduction (Figure 2C) (Pomeroy et al., 2020) resulted in 17% (300,000 multiplicities of infection [MOIs]) and 19% (500,000 MOIs) mCherry-positive NK cells (Figure 3A). We further expanded these cells for 1 week using FC21, enriched the mCherry-positive cells by fluorescence-activated cell sorting (FACS), and did not see any reduction in the expression level of mCherry during an additional 30 days of expansion (Figures 3A–3C), demonstrating stable integration.

Improved gene insertion by using self-complementary AAV6 and Cas9/RNP

After transduction, scAAV vectors can acquire the necessary double-stranded state in a shorter time frame than ssAAV, which may impact the efficiency of gene insertion. Due to the size limitation of packaging transgenes in scAAV, we designed HAs of varying lengths to minimize the size needed for scAAV backbones. Hence, HAs of 30, 300, 500, and 1,000 bp length for the right and 30, 300, 500, and 800 bp for the left (Figure 2A) were cloned with mCherry into the scAAV backbone and packaged into AAV6 capsid. We then followed the same steps as for the ssAAV above to electroporate and transduce the day 7 expanded NK cells. scAAV with HAs $\geq$300 bp showed markedly increased efficiency of gene transfer at >80% (Figures 3A and 3B). Stable mCherry gene expression was observed for at least 3 weeks of additional NK cell expansion (Figure 3C). When we used the same approach in freshly isolated NK cells, mCherry expression was significantly lower (1.13% for 800 bp ssAAV6; 2.9% for self-complementary [sc] 300 bp scAAV6; Figure S2A).

CRISPaint for gene insertion in NK cells

To overcome the complexity of HA optimization seen in HDR-directed gene insertion, we tested a homology-independent gene-insertion approach called CRISPaint. For the CRISPaint DNA templates, we incorporated double Cas9-targeting sequences of AAVS1 (PAMgPAMg) around the mCherry transgene but within the inverted terminal repeats (ITRs) of scAAV and packaged it into AAV6 (Figure 2B). Two days after electroporation and transduction, we performed flow cytometry to assess mCherry expression in NK cells. The cells that were electroporated and transduced with 300,000 MOIs of scAAV6 delivering CRISPaint PAMgPAMg were found to be up to 6% mCherry positive. We further sorted and enriched these NK cells and expanded them for 30 days and saw no decline in the percentage that were mCherry positive (Figures 3B and 3C). Although we saw lower efficiency of gene integration using CRISPaint compared with HDR-directed gene insertion, this method may still be useful because it allows integration into a user-defined locus without designing HAs.

Generation of human primary CD33-CAR NK cells

We tested two CAR constructs comprising the same CD33-targeting single-chain variable fragment (scFv) but with a CD4 transmembrane domain and CD28/CD3ζ signaling domain (Gen2) or an NKG2D transmembrane domain and 2B4/CD3ζ signaling domain (Gen4v2) (Li et al., 2018) (Figures 4A and 4B). The CAR constructs were too large for suitable packaging into the scAAV backbone, so they were cloned into the ssAAV backbone with the largest possible HAs of 600 bp. To improve the expression of the CARs, we also incorporated a murine leukemia virus-derived promoter (MND) before the start codon of the CARs instead of the splice acceptor. As with the mCherry vectors, these were packaged into the AAV6 capsid. Seven days after electroporation and transduction, we detected up to 78% CD33 CAR-expressing NK cells (mean 59.3% for Gen2 and 60% for Gen4v2). Of note, the CD33CAR-Gen2 resulted in a higher level of expression on NK cells compared with Gen4v2 (Figures 4C, 4D, and S2B). We expanded the cells for another week (day 14) and observed no significant reduction in CAR expression (Figure 4E and S2C) or proliferative potential (Figure 4F), suggesting that neither the AAV6 transduction event nor the CAR expression impacted NK cell proliferation or survival. Efficient CAR integration (>60%) was also observed with MOIs as low as 10,000 (Figure S3), and toxicity of the AAV6 transduction was not observed across the MOIs tested.

Detection of the transgene at the targeted AAVS1 locus and unintended insertion sites

Using PCR with primers to flanking and inter-transgenic regions (Figure 5A; Table S1), we confirmed the DNA integration of the transgenes (Figure 5B). Additionally, targeted locus amplification (TLA) was used for whole-genome mapping of CD33CAR-Gen2 integration in CAR-expressing NK cells with a sensitivity of detecting random integrations of more than 5%. As seen in Figure 5C, the vector has integrated as intended in human chromosome chr19: 55,115,754–55,115,767, which is in intron 1 of PPP1R12C. Other integration sites were observed between chr19: 55,115,155–55,116,371, which is also in intron 1 of PPP1R12C (Figures S4A and S6; Table S1). Sequence variants and structural variants were identified in the covered regions (Figure S4B; Data S1). There was no indication of a dominant secondary off-target integration site. One sequence variant and four structural variants were detected (Table S2). The frequency of detection suggests this variant was present within the AAV6 vector itself. Overall, the TLA demonstrated high prevalence of vector integration at the targeted location in chromosome 19, with low-level random integrations identified throughout the genome.

Figure 2. Constructs, integration process, and method workflow for gene insertion through HR and CRISPaint

(A) Constructs and integration process through HR. Cas9/RNP introduces a DSB in AAVS1, after which DNA encoding a gene of interest can be integrated through HR by varying lengths of HAs. The schematics show the construct designs for integration of DNA encoding mCherry with HAs between 30 and 1,000 bp for Cas9-targeting site in AAVS1 and cloned in ssAAV6 and/or scAAV6 backbone.

(B) Top, construct design for insertion of DNA encoding mCherry through CRISPaint and cloned in scAAV. Bottom, schematics showing the integration process for CRISPaint gene insertion through homology-independent DNA-repair pathway.

(C) Schematics of workflow to electroporate Cas9/RNP and transduce AAV6 for gene delivery into NK cells.

A

Cas9 + gRNA AAVS1	-	+	-	+	+
AAV6	-	-	ssAAV	ssAAV	ssAAV
MOI	0	0	300K	300K	500K
Homology arms	0	0	800 bp	800 bp	800 bp

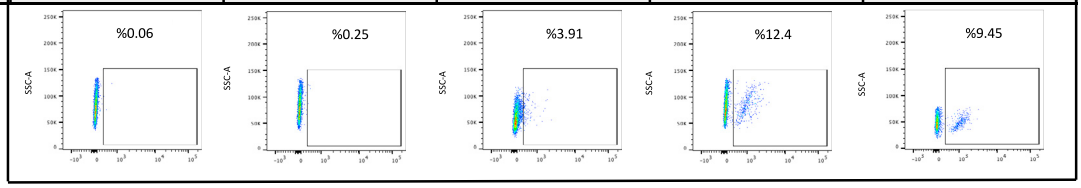

Cas9 + gRNA AAVS1	+	+	+	+	+
AAV6	scAAV	scAAV	scAAV	scAAV	scAAV
MOI	300K	300K	300K	300K	300K
Homology arms	CRISPaint	30 bp	300 bp	500 bp	800 bp

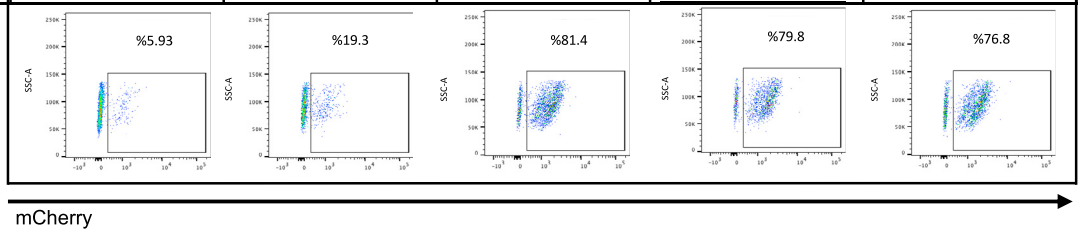

B

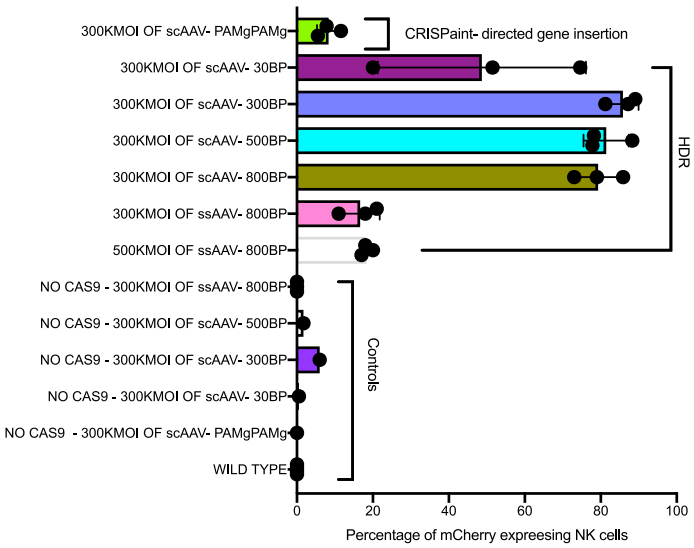

C

Cas9 + gRNA AAVS1	+	+
AAV6	ssAAV	scAAV
MOI	500K	300K
Homology arms	800 bp	CRISPaint

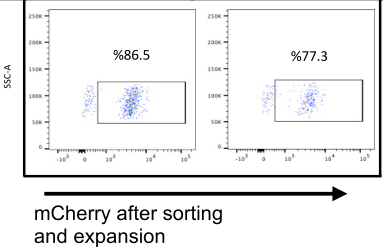

Figure 3. Combination of AAV6 and Cas9/RNP results in efficient generation of mCherry-expressing NK cells

(A) Representative flow cytometry of human primary NK cells expressing mCherry 2 days after Cas9/RNP electroporation and AAV6 transduction (MOI = 3-5 × 10^5).

(B) Efficiency of Cas9/RNP and AAV6-mediated mCherry expression in human primary NK cells through HR and CRISPaint (n = 3). Data are shown as mean ± SD.

(C) mCherry expression in NK cells after enrichment and 2 additional weeks of expansion.

CD33CAR constructs cloned in ssAAV

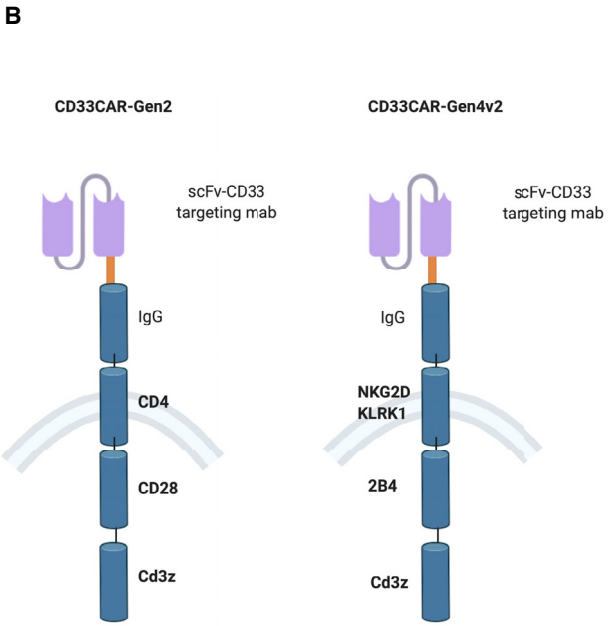

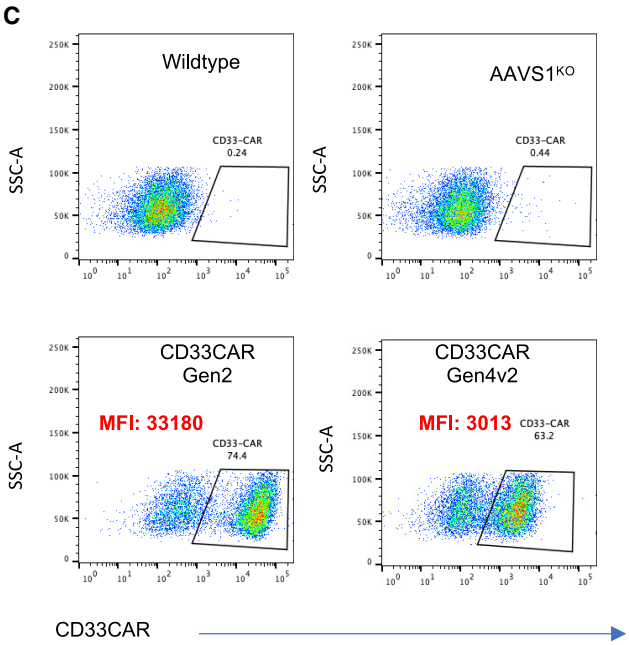

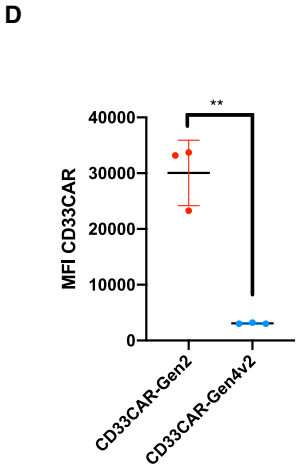

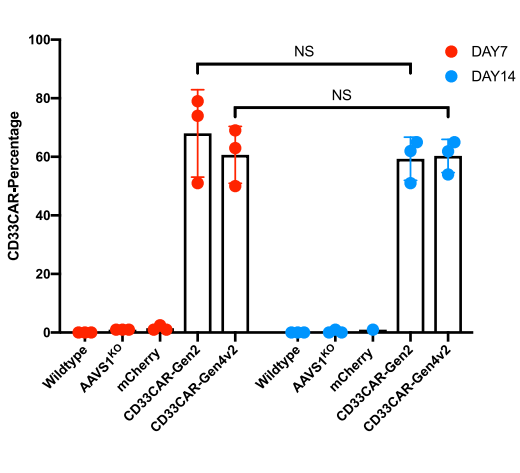

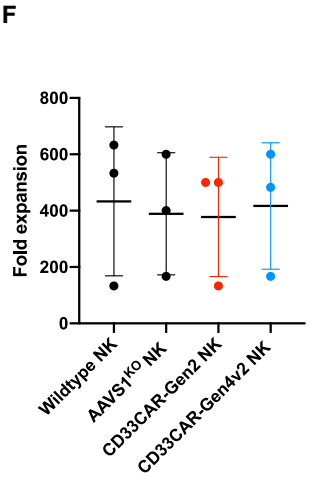

(legend on next page)

Human primary CAR-NK cells have enhanced antitumor activity

To determine whether the CD33CAR enhanced NK cell killing of AML cells, we performed a calcein-AM-based cytotoxicity assay with two CD33-expressing AML cell lines (Kasumi-1 and HL60) and one patient-derived sample (AML10) (Figure S5A) using CD33CAR-NK cells generated from three different healthy individuals. CD33CAR-gen2 and -gen4v2 NK cells showed a significantly higher degranulation and target cell lysis when co-cultured with Kasumi-1 or HL60 cell lines compared with wild-type or *AAVS1*^{KO} NK cells (Figures 6A–6D). Importantly, we showed significantly higher antitumor activity of CD33CAR NK cells against *AML-10,* a primary human AML sample derived from a patient with relapsed and refractory AML (Figure 6E) (Dutour et al., 2012; Somanchi et al., 2011). Overall, CD33CAR-Gen2 NK showed better cytotoxicity compared with CD33CAR-Gen4v2 NK cells. Due to the higher antitumor activity of CD33CAR-Gen2, we only used these CAR-NK cells for the rest of the functional assessments. Using real-time assessment of cytotoxicity (xCELLigence), we showed that CD33CAR-Gen2-NK cells kill the CD33-expressing AML cells more completely and with faster kinetics than the same donor wild-type (WT) NK cells (Figures 6F and S5B–S5E). CD33CAR-Gen2 NK cells also showed significantly higher secretion of interferon gamma (IFNγ) and tumor necrosis factor alpha (TNF-α) when co-cultured with Kasumi-1 compared with non-modified NK cells (Figure S4F).

Mass cytometry showed enhanced killing and specificity of CD33CAR-NK cells against AML

We previously used the combination of pRb and cleaved PARP (Behbehani et al., 2012; Devine et al., 2021) to enable very accurate detection of dead or dying cells in mass cytometry with a wide variety of other extracellular and intracellular markers. Here, we used the same approach to measure the ability of CAR-NK cells to kill AML cells. WT or CD33Gen2-CAR NK cells generated from one donor were co-cultured with primary AML and then assessed for viability across multiple cell populations. Four main populations (Figure 6G) were identified by both manual gating and SPADE clustering: live proliferating NK cells, quiescent NK cells, live proliferating AML cells, and dying AML cells. At 3 h, control primary AML cells were ~66% viable, whereas viability decreased to 56% when co-cultured with WT-NK cells and only 21% when co-cultured with CD33CAR NK cells. At 24 h, control primary AML cells recovered to 89% viability compared with 76% when co-cultured with WT-NK cells and only 42% when co-cultured with CD33CAR NK cells. At 3 h, the surviving AML cells had a 20-fold reduction in CD33 expression when cultured with the CD33CAR NK cells (median of 104 counts down to 5 counts), while there was minimal change in CD33 expression in the WT NK cell co-culture (median of 104 counts down to 87 counts). This difference persisted at 24 h, at which time the median CD33 counts were 25 for CD33CAR NK cells, 118 for WT NK cells, and 120 in control AML without NK cells. Co-culture with AML also increased NK activation markers (CD69, CD99, CD71, NKG2D, CD16, and CD45) at 24 h compared with the NK cells cultured alone (data not shown). The CD33CAR NK cells had lower levels of activation markers at baseline that increased more with co-culture. Together, these data show that CD33CAR-NK cells specifically target CD33-expressing AML and are more activated by the AML targets compared with WT-NK cells (Figure 6G).

DISCUSSION

Gene transfer in NK cells has been challenging. Despite some progress having been made to transduce NK cells with lentiviral and retroviral vectors to generate CAR-NK cells, the efficiency of these methods remains relatively low. Here, we report a highly efficient method for site-directed gene integration into human primary NK cells using a combination of electroporation of Cas9/RNP and ssAAV6 or scAAV6 gene delivery through HDR and homology-independent gene insertion (CRISPaint). We also show that the expression level of genes regulating HDR and NHEJ pathways in human NK cells generally increase during expansion, with FC21 resulting in improved conditions for site-directed gene insertion. We also demonstrated that AAVS1 could host and express exogenous genes in a very highly efficient level, as shown previously in T cells and NK cells (Pomeroy et al., 2020). Furthermore, we showed that a range of HAs from 30–1,000 bp can be used for gene insertion into the AAVS1 locus in NK cells but that the shortest optimal length is at 300 bp when used in scAAV6. We observed no difference between WT and CRISPR-modified AAVS1^{KO} NK cells in degranulation or cytotoxicity against AML cell lines, which suggests that genome modifications at this locus do not interfere with NK cell function (Figure 6C, S1B, S5B, and S5C). Although less efficient, CRISPaint gene insertion may be useful for tagging endogenous genes and therefore may be useful for biologic studies in NK cells.

Transcripts that are delivered via AAV vectors can be packaged as a linear ssDNA with a length of approximately 4.7 kb (ssAAV) or as linear scDNA (scAAV). The benefit of the scAAV vector is that it contains a mutated ITR, which is required for

Figure 4. Successful generation of CD33CAR-expressing NK cells using combination of Cas9/RNP and AAV6

(A) Schematic of anti-CD33 CAR constructs (Gen2 and Gen4v2) with HAs for AAVS1-targeting site and cloned in ssAAV.

(B) Schematic of CAR protein structural design.

(C) Representative flow cytometry showing the expression level of CD33CAR on NK cells 7 days after Cas9/RNP electroporation and AAV6 transduction (MOI = 3×10^5).

(D) Mean fluorescence intensity (MFI) of CD33CAR expression for Gen2 versus Gen4v2 ($p = 0.0014$, unpaired t test).

(E) CD33CAR expression level on NK cells 7 and 14 days after transduction and electroporation (n = 3, n.s. from two-way ANOVA adjusted for multiple comparisons).

(F) Fold expansion of CD33CAR-expressing NK cells on feeder cells for 14 days starting from 3×10^5 cells (n = 3, n.s. from one-way ANOVA adjusted for multiple comparisons). Data are shown as mean ± SD. Significant p values indicated are from individual ratio paired t tests and are not adjusted for multiple comparisons. **$p < 0.01$.

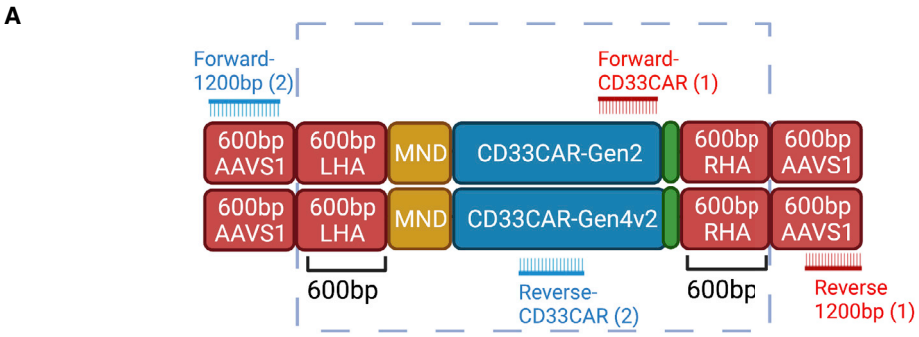

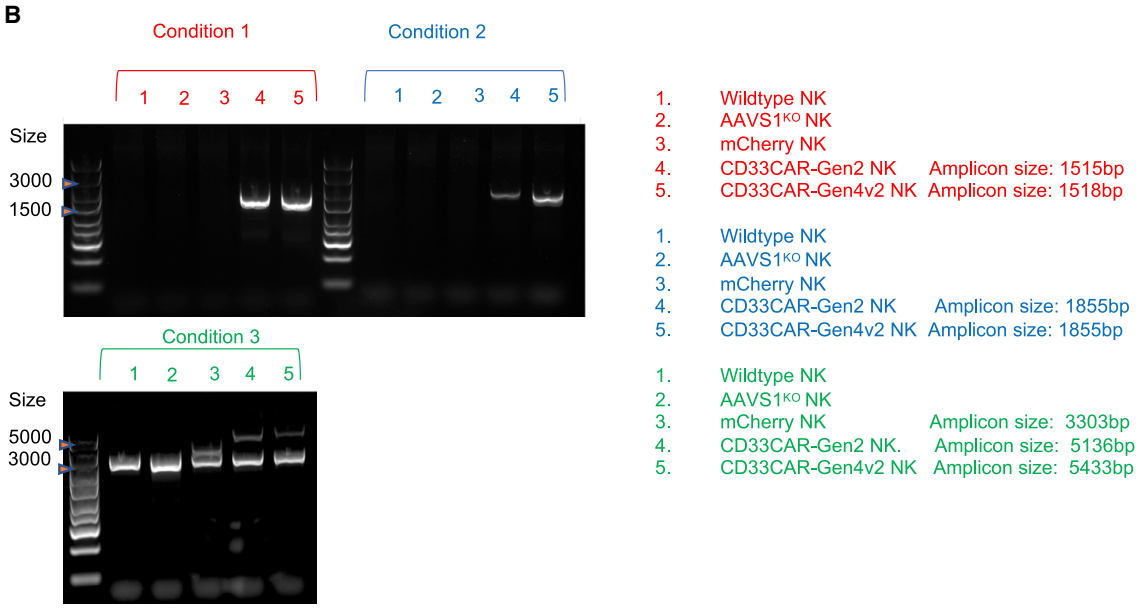

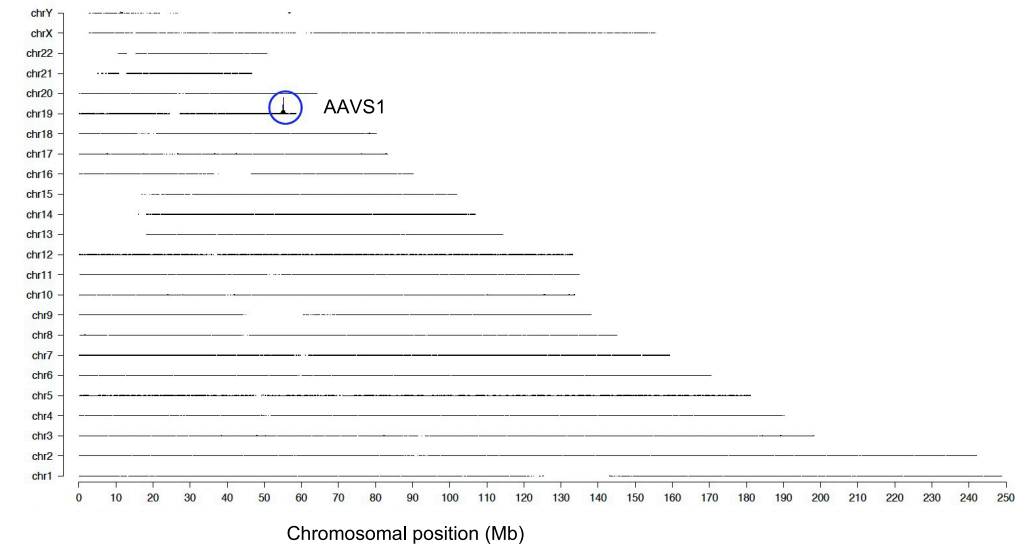

(legend on next page)

replication and helps to bypass rate-limiting steps of second-strand generation compared with ssDNA vectors (McCarty, 2008). Due to the limitation in the packaging capacity of scAAV, we designed 30, 300, 500, and 800–1,000 bp of HAs for the right and left side of the Cas9-targeting site to find the most optimal length of HAs and to provide possible lengths of HAs to be chosen based on the size of transgenes by researchers (Figure 2A). Additionally, due to limitations in packaging capacity compared with ssAAV, scAAV is not suitable for larger transgenes such as CARs targeting CD33 (McCarty, 2008). Therefore, based on the size of transgenes, we designed and tested both ssAAV and scAAV, which provides a wide range of options for gene insertion in primary NK cells.

Since designing HAs is a time-consuming procedure and requires multiple optimizations, we also investigated the CRISPaint approach, a homology-independent method for gene insertion or tagging. In this method, the same Cas9-targeting site, including the CRISPR RNA (crRNA) and protospacer adjacent motif (PAM) sequence, is provided in the DNA template encoding the gene of interest. Upon the introduction of the Cas9 complex, both template and genomic DNA will be cut simultaneously. As a result, the CRISPaint template will be presented as a linearized double-stranded DNA that can be integrated through non-HR machinery (Figure 2B) (Suzuki et al., 2016; Schmid-Burgk et al., 2016). We also used the combination of Cas9/RNP and AAV6 gene delivery and generated two different human primary CD33CAR NK cells with enhanced anti-AML activity. Here we show the feasibility of using Cas9/RNP and AAV to generate CAR-NK cells using two different CAR constructs targeting CD33. Differences in the transmembrane domains of the CARs may explain their different surface-expression levels since both CARs are inserted into the same locus with the same promoter, reducing epigenetic variability in expression seen with methods that result in random insertion sites. We did not observe significant differences in their anti-AML activity, but the different CAR constructs warrant further investigation to better understand the biologic consequences on expression and effector function in NK cells, which might be different from that in T cells. Although successful NK cell transduction has been reported using non-viral and feeder-cell-free approaches (Huang et al., 2021), transduction efficiency, silencing of expression, cell death, and obtaining sufficient numbers of NK cells after gene editing continues to be a hurdle. Here, we show that the combination of activation/expansion on IL-21-expressing feeder cells, Cas9/RNP, and AAV resulted in highly efficient CAR expression and production of large numbers of gene-modified NK cells applicable to cancer immunotherapy. This manufacturing method can also serve as a platform to answer broader questions on the utility, design, persistence, and function of CAR-NK cells in screening assays and *in vivo* models that require large numbers of modified cells. Overall, our method has wide potential for applications in immunology, cancer immunotherapy, and basic biology of NK cells.

Limitations of the study

Here, we show that the efficiency of modifying freshly isolated human primary CAR NK cells in their naive stage is low. Thus, to achieve high-efficiency modification, the NK cells must be activated/expanded first to induce DNA-repair machinery. Our previously published approach for activation/expansion of human primary NK cells with FC21 worked well for this, and we did not broadly explore other methods for upregulation of DNA-repair pathways. Our FC21 activation/expansion approach has been applied to canine and non-human primate NK cells but does not work well for murine NK cells, and therefore, this overall method may not directly apply to murine NK cell research. AAV vectors have a more limited payload than most other vectors, which may limit the applicability of this method. For highest efficiency, this approach requires the inclusion of HAs in the vector design, further reducing the size of the genes that can be inserted.

STAR★METHODS

Detailed methods are provided in the online version of this paper and include the following:

- KEY RESOURCES TABLE
- RESOURCE AVAILABILITY
  - Lead contact
  - Materials availability
  - Data and code availability
- EXPERIMENTAL MODEL AND SUBJECT DETAILS
  - Cell lines and primary cultures
- METHOD DETAILS
  - Human NK cell purification and expansion
  - ATAC-seq assay
  - Cas9/RNP electroporation for targeting AAVS1 in NK cells
  - Inference of CRISPR Edits (ICE) mutation detection assay
  - RNA-seq sample preparation and sequencing
  - AAV6 production
  - Combining Cas9/RNP and AAV6 to generate mCherry and CAR NK cells

Figure 5. Integration of the transgene in AAVS1 locus confirmed by PCR and TLA

(A) Schematic of PCR primers designed inside and outside of CD33CARs encoding DNA and integrated in AAVS1.

(B) Amplicons were amplified and visualized on 1% agar gel from NK cells to specifically identify the CD33CAR gene inserted at the AAVS1 locus (PCR condition 1 [primers forward-1 and reverse-1] and PCR condition 2 [primers forward-2 and reverse-2]) and confirmed by amplifying the AAVS1 locus outside of the transgenes (PCR condition 3 [primers forward-2 and reverse-1]; Table S1).

(C) TLA sequence coverage across the human genome in CAR-NK cells expanded for 14 days using primers designed to detect integration of CD33CAR-Gen2. The chromosomes are indicated on the y axis and the chromosomal position on the x axis. A single integration site was identified above background, shown encircled in blue.

See also Table S1 and Data S1.

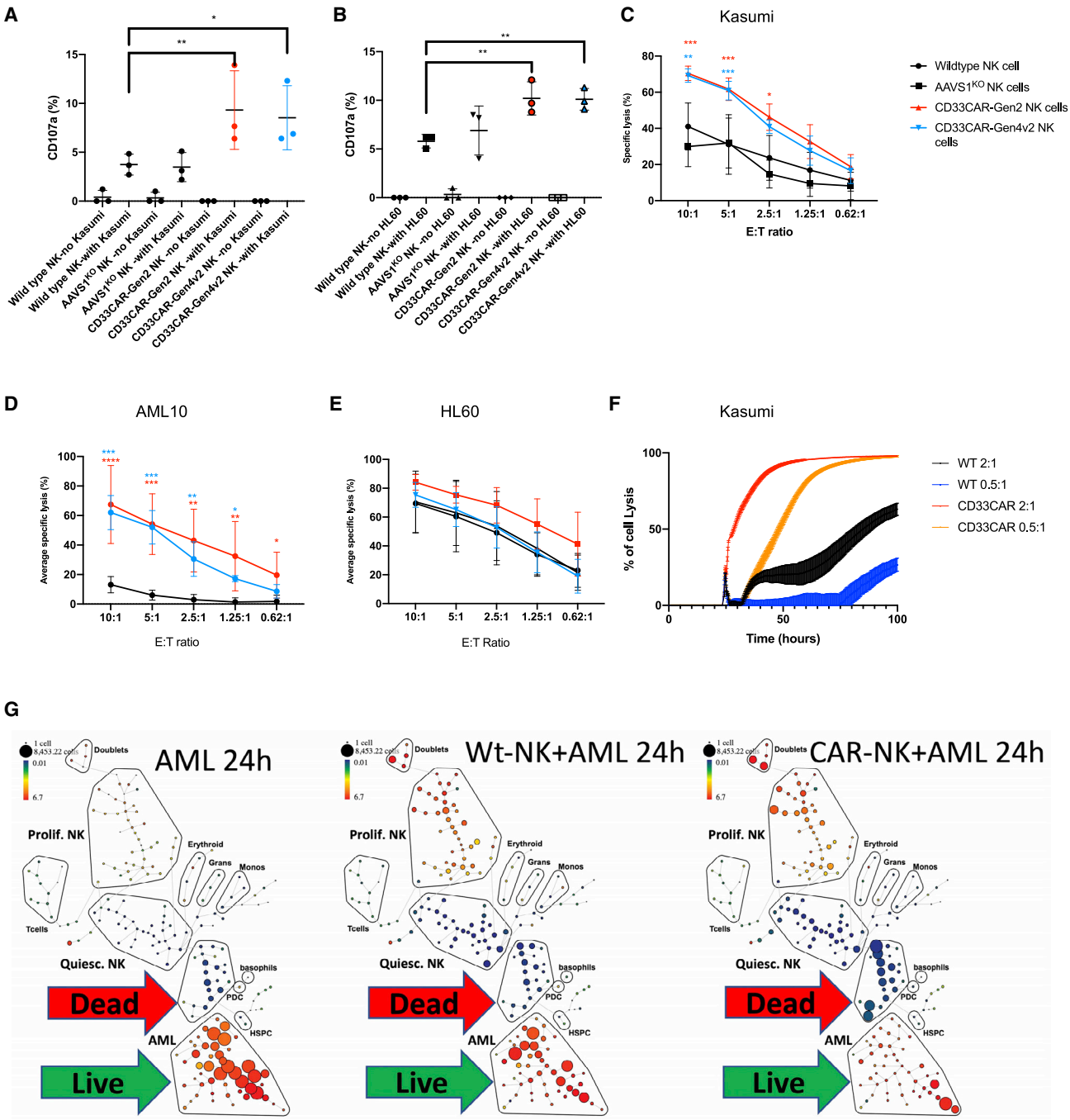

Figure 6. CD33CAR NK cells have enhanced anti-AML activity

(A and B) CD33CAR NK cells degranulate significantly higher than wild-type NK cells when co-cultured with *Kasumi-1* (A) and *HL60* (B).

(C) Expressing CD33CAR on NK cells also enhances overall antitumor activity of NK cells against *Kasumi-1* in three donors.

(D and E) This enhanced cytotoxic activity was also observed against *AML-10* primary cells (D) but not against HL-60 (E).

(F) The superior antitumor activity of the CD33CAR-Gen2 was also observed in a long-term cytotoxicity assay using xCelligence against Kasumi.

(G) Cytometry by time of flight (CyTOF) analysis showed killing by the CD33CAR Gen2 NK cells of specific subsets of AML that were resistant to wild-type NK cells.

*p < 0.05, **p < 0.01, ***p < 0.001, or ****p < 0.0001, by two-way ANOVA adjusted for multiple comparisons.

- Flow cytometry for detection of CAR-NK cells and cancer cells
- Cytotoxicity assay
- CD107a staining
- Cytokine secretion assay
- PCR-based detection of transgenes integration
- Targeted locus amplification (TLA)
- Real-time potency assessment for suspension target cells killed by WT and CD33CAR NK cells
- AML-NK cell Co-Culture
- Mass cytometry staining and analysis

● QUANTIFICATION AND STATISTICAL ANALYSIS

SUPPLEMENTAL INFORMATION

Supplemental information can be found online at https://doi.org/10.1016/j.crmeth.2022.100236.

ACKNOWLEDGMENTS

This work was supported by funding from the CancerFree KIDS Pediatric Cancer Research Alliance (M.N.K.), the Hyundai Hope on Wheels Foundation (D.A.L.), and the NIH-NCI (U54-CA232561, D.A.L.). We thank the Institute for Genomic Medicine at Nationwide Children's Hospital for their assistance with nucleic acid sequencing. Schematics were created with https://biorender.com.

AUTHOR CONTRIBUTIONS

M.N.K. and D.A.L. conceived of the project; S.L., K.Y., B.S.M., K.M., G.K.B., M.d.S.F.P., and D.A.L. designed the experiments; M.N.K., S.L., K.Y., N.C., E.E., Y.S., M.S., R.D.D., J.M.L., and K.S. performed the experiments; M.N.K., K.Y., B.S.M., G.K.B., and D.A.L. analyzed and interpreted the data; and M.N.K., K.Y., B.S.M., M.S., and D.A.L. prepared the manuscript.

DECLARATION OF INTERESTS

D.A.L. reports stock from Courier Therapeutics, personal fees and stock options from Caribou Biosciences, and membership on the NIH Novel and Exception Therapies and Research Advisory Committee (NExTRAC) unrelated to the submitted work. D.A.L. also reports membership on the scientific advisory board and consulting, licensing, and royalty fees from Kiadis Pharma related to patents US62/825,007; US63/105,722; US62/928,524; PCT-US2019/032,670; PCT-US2018/020187; WO2019/222,503-A1; PCT-US2020/018,384; US62/805,394; US62/987,935; US62/900,245; and US62/815,625. M.N.K. reports consulting, licensing, and royalty fees from Kiadis Pharma related to patents US62/825,007, WO2019/222,503A1, US63/105,722, PCT-US2020/02545, US63/018,108, US62/928,524, and US62/987,935. B.S.M. is founder of and has sponsored research with Catamaran Bio and patent WO2017/214,569A1. K.M. and S.L. report licensing and royalty fees from Kiadis Pharma related to patent PCT-US2020/025,454. N.C. reports licensing and royalty fees from Kiadis Pharma related to patent PCT-US2018/020,187.

Received: June 3, 2021
Revised: October 8, 2021
Accepted: May 23, 2022
Published: June 13, 2022

REFERENCES

Behbehani, G.K., Bendall, S.C., Clutter, M.R., Fantl, W.J., and Nolan, G.P. (2012). Single-cell mass cytometry adapted to measurements of the cell cycle. Cytometry *81*, 552–566. https://doi.org/10.1002/cyto.a.22075.

Buenrostro, J.D., Giresi, P.G., Zaba, L.C., Chang, H.Y., and Greenleaf, W.J. (2013). Transposition of native chromatin for fast and sensitive epigenomic profiling of open chromatin, DNA-binding proteins and nucleosome position. Nat. Methods *10*, 1213–1218. https://doi.org/10.1038/nmeth.2688.

Cerignoli, F., Abassi, Y.A., Lamarche, B.J., Guenther, G., Santa Ana, D., Guimet, D., Zhang, W., Zhang, J., and Xi, B. (2018). In vitro immunotherapy potency assays using real-time cell analysis. PLoS One *13*, e0193498. https://doi.org/10.1371/journal.pone.0193498.

Chen, C.C., Feng, W., Lim, P.X., Kass, E.M., and Jasin, M. (2018). Homology-directed repair and the role of BRCA1, BRCA2, and related proteins in genome integrity and cancer. Annu. Rev. Cell Biol. *2*, 313–336. https://doi.org/10.1146/annurev-cancerbio-030617-050502.

de Vree, P.J.P., De Wit, E., Yilmaz, M., Van De Heijning, M., Klous, P., Verstegen, M.J.A.M., Wan, Y., Teunissen, H., Krijger, P.H.L., Geeven, G., et al. (2014). Targeted sequencing by proximity ligation for comprehensive variant detection and local haplotyping. Nat. Biotechnol. *32*, 1019–1025. https://doi.org/10.1038/nbt.2959.

Denman, C.J., Senyukov, V.V., Somanchi, S.S., Phatarpekar, P.V., Kopp, L.M., Johnson, J.L., Singh, H., Hurton, L., Maiti, S.N., Huls, M.H., et al. (2012). Membrane-bound IL-21 promotes sustained ex vivo proliferation of human natural killer cells. PLoS One *7*, e30264. https://doi.org/10.1371/journal.pone.0030264.

Devine, R.D., Alkhalaileh, H.S., Lyberger, J.M., and Behbehani, G.K. (2021). Alternative methods of viability determination in single cell mass cytometry. Cytometry *99*, 1042–1053. https://doi.org/10.1002/cyto.a.24308.

Dutour, A., Marin, V., Pizzitola, I., Valsesia-Wittmann, S., Lee, D., Yvon, E., Finney, H., Lawson, A., Brenner, M., Biondi, A., et al. (2012). In vitro and in vivo antitumor effect of anti-CD33 chimeric receptor-expressing EBV-CTL against CD33 acute myeloid leukemia. Adv. Hematol. *2012*, 683065. https://doi.org/10.1155/2012/683065.

Eyquem, J., Mansilla-Soto, J., Giavridis, T., van der Stegen, S.J.C., Hamieh, M., Cunanan, K.M., Odak, A., Gonen, M., and Sadelain, M. (2017). Targeting a CAR to the TRAC locus with CRISPR/Cas9 enhances tumour rejection. Nature *543*, 113–117. https://doi.org/10.1038/nature21405.

Finck, R., Simonds, E.F., Jager, A., Krishnaswamy, S., Sachs, K., Fantl, W., Pe'er, D., Nolan, G.P., and Bendall, S.C. (2013). Normalization of mass cytometry data with bead standards. Cytometry *83*, 483–494. https://doi.org/10.1002/cyto.a.22271.

Foltz, J.A., Moseman, J.E., Thakkar, A., Chakravarti, N., and Lee, D.A. (2018). TGFbeta imprinting during activation promotes natural killer cell cytokine hypersecretion. Cancers *10*, 423. https://doi.org/10.3390/cancers10110423.

Foust, K.D., Salazar, D.L., Likhite, S., Ferraiuolo, L., Ditsworth, D., Ilieva, H., Meyer, K., Schmelzer, L., Braun, L., Cleveland, D.W., and Kaspar, B.K. (2013). Therapeutic AAV9-mediated suppression of mutant SOD1 slows disease progression and extends survival in models of inherited ALS. Mol. Ther. *21*, 2148–2159. https://doi.org/10.1038/mt.2013.211.

Gleason, M.K., Ross, J.A., Warlick, E.D., Lund, T.C., Verneris, M.R., Wiernik, A., Spellman, S., Haagenson, M.D., Lenvik, A.J., Litzow, M.R., et al. (2014). CD16xCD33 bispecific killer cell engager (BiKE) activates NK cells against primary MDS and MDSC CD33+ targets. Blood *123*, 3016–3026. https://doi.org/10.1182/blood-2013-10-533398.

He, X., Tan, C., Wang, F., Wang, Y., Zhou, R., Cui, D., You, W., Zhao, H., Ren, J., and Feng, B. (2016). Knock-in of large reporter genes in human cells via CRISPR/Cas9-induced homology-dependent and independent DNA repair. Nucleic Acids Res. *44*, e85. https://doi.org/10.1093/nar/gkw064.

Hsiau, T., Maures, T., Waite, K., Yang, J., Kelso, R., Holden, K., and Stoner, R. (2018). Inference of CRISPR Edits from sanger trace data. Preprint at bioRxiv. https://doi.org/10.1101/251082.

Huang, R.S., Lai, M.C., Shih, H.A., and Lin, S. (2021). A robust platform for expansion and genome editing of primary human natural killer cells. J. Exp. Med. *218*. https://doi.org/10.1084/jem.20201529.

Kim, M.Y., Yu, K.R., Kenderian, S.S., Ruella, M., Chen, S., Shin, T.H., Aljanahi, A.A., Schreeder, D., Klichinsky, M., Shestova, O., et al. (2018). Genetic

inactivation of CD33 in hematopoietic stem cells to enable CAR T cell immunotherapy for acute myeloid leukemia. Cell *173*, 1439–1453.e19. https://doi.org/10.1016/j.cell.2018.05.013.

Kotecha, N., Krutzik, P.O., and Irish, J.M. (2010). Web-based analysis and publication of flow cytometry experiments. Curr. Protoc. Cytom. Chapter 10, Unit10 17. https://doi.org/10.1002/0471142956.cy1017s53.

Lee, D.A., Verneris, M.R., and Campana, D. (2010). Acquisition, preparation, and functional assessment of human NK cells for adoptive immunotherapy. Methods Mol. Biol. *651*, 61–77. https://doi.org/10.1007/978-1-60761-786-0_4.

Li, K., Wang, G., Andersen, T., Zhou, P., and Pu, W.T. (2014). Optimization of genome engineering approaches with the CRISPR/Cas9 system. PLoS One *9*, e105779. https://doi.org/10.1371/journal.pone.0105779.

Li, Y., Hermanson, D.L., Moriarity, B.S., and Kaufman, D.S. (2018). Human iPSC-derived natural killer cells engineered with chimeric antigen receptors enhance anti-tumor activity. Cell Stem Cell *23*, 181–192.e5. https://doi.org/10.1016/j.stem.2018.06.002.

Liu, E., Marin, D., Banerjee, P., Macapinlac, H.A., Thompson, P., Basar, R., Nassif Kerbauy, L., Overman, B., Thall, P., Kaplan, M., et al. (2020). Use of CAR-transduced natural killer cells in CD19-positive lymphoid tumors. N. Engl. J. Med. *382*, 545–553. https://doi.org/10.1056/NEJMoa1910607.

Liu, J., Zhou, G., Zhang, L., and Zhao, Q. (2019). Building potent chimeric antigen receptor T cells with CRISPR genome editing. Front. Immunol. *10*, 456. https://doi.org/10.3389/fimmu.2019.00456.

MacLeod, D.T., Antony, J., Martin, A.J., Moser, R.J., Hekele, A., Wetzel, K.J., Brown, A.E., Triggiano, M.A., Hux, J.A., Pham, C.D., et al. (2017). Integration of a CD19 CAR into the TCR alpha chain locus streamlines production of allogeneic gene-edited CAR T cells. Mol. Ther. *25*, 949–961. https://doi.org/10.1016/j.ymthe.2017.02.005.

Mali, P., Yang, L., Esvelt, K.M., Aach, J., Guell, M., Dicarlo, J.E., Norville, J.E., and Church, G.M. (2013). RNA-guided human genome engineering via Cas9. Science *339*, 823–826. https://doi.org/10.1126/science.1232033.

Mani, R., Rajgolikar, G., Nunes, J., Zapolnik, K., Wasmuth, R., Mo, X., Byrd, J.C., Lee, D.A., Muthusamy, N., and Vasu, S. (2020). Fc-engineered anti-CD33 monoclonal antibody potentiates cytotoxicity of membrane-bound interleukin-21 expanded natural killer cells in acute myeloid leukemia. Cytotherapy *22*, 369–376. https://doi.org/10.1016/j.jcyt.2020.02.001.

McCarty, D.M. (2008). Self-complementary AAV vectors; advances and applications. Mol. Ther. *16*, 1648–1656. https://doi.org/10.1038/mt.2008.171.

Mendell, J.R., Al-Zaidy, S., Shell, R., Arnold, W.D., Rodino-Klapac, L.R., Prior, T.W., Lowes, L., Alfano, L., Berry, K., Church, K., et al. (2017). Single-dose gene-replacement therapy for spinal muscular atrophy. N. Engl. J. Med. *377*, 1713–1722. https://doi.org/10.1056/NEJMoa1706198.

Moseman, J.E., Foltz, J.A., Sorathia, K., Heipertz, E.L., and Lee, D.A. (2020). Evaluation of serum-free media formulations in feeder cell-stimulated expansion of natural killer cells. Cytotherapy *22*, 322–328. https://doi.org/10.1016/j.jcyt.2020.02.002.

Naeimi Kararoudi, M., Dolatshad, H., Trikha, P., Hussain, S.R.A., Elmas, E., Foltz, J.A., Moseman, J.E., Thakkar, A., Nakkula, R.J., Lamb, M., et al. (2018). Generation of knock-out primary and expanded human NK cells using Cas9 ribonucleoproteins. JoVE, 58237. https://doi.org/10.3791/58237.

Naeimi Kararoudi, M., Nagai, Y., Elmas, E., De Souza Fernandes Pereira, M., Ali, S.A., Imus, P.H., Wethington, D., Borrello, I.M., Lee, D.A., and Ghiaur, G. (2020a). CD38 deletion of human primary NK cells eliminates daratumumab-induced fratricide and boosts their effector activity. Blood *136*, 2416–2427. https://doi.org/10.1182/blood.2020006200.

Naeimi Kararoudi, M., Tullius, B.P., Chakravarti, N., Pomeroy, E.J., Moriarity, B.S., Beland, K., Colamartino, A.B.L., Haddad, E., Chu, Y., Cairo, M.S., and Lee, D.A. (2020b). Genetic and epigenetic modification of human primary NK cells for enhanced antitumor activity. Semin. Hematol. *57*, 201–212. https://doi.org/10.1053/j.seminhematol.2020.11.006.

Oceguera-Yanez, F., Kim, S.I., Matsumoto, T., Tan, G.W., Xiang, L., Hatani, T., Kondo, T., Ikeya, M., Yoshida, Y., Inoue, H., and Woltjen, K. (2016). Engineering the AAVS1 locus for consistent and scalable transgene expression in human iPSCs and their differentiated derivatives. Methods *101*, 43–55. https://doi.org/10.1016/j.ymeth.2015.12.012.

Pomeroy, E.J., Hunzeker, J.T., Kluesner, M.G., Lahr, W.S., Smeester, B.A., Crosby, M.R., Lonetree, C.L., Yamamoto, K., Bendzick, L., Miller, J.S., et al. (2020). A genetically engineered primary human natural killer cell platform for cancer immunotherapy. Mol. Ther. *28*, 52–63. https://doi.org/10.1016/j.ymthe.2019.10.009.

Qiu, P., Simonds, E.F., Bendall, S.C., Gibbs, K.D., Jr., Bruggner, R.V., Linderman, M.D., Sachs, K., Nolan, G.P., and Plevritis, S.K. (2011). Extracting a cellular hierarchy from high-dimensional cytometry data with SPADE. Nat. Biotechnol. *29*, 886–891. https://doi.org/10.1038/nbt.1991.

Rahman, A.H., Tordesillas, L., and Berin, M.C. (2016). Heparin reduces nonspecific eosinophil staining artifacts in mass cytometry experiments. Cytometry *89*, 601–607. https://doi.org/10.1002/cyto.a.22826.

Ran, F.A., Hsu, P.D., Wright, J., Agarwala, V., Scott, D.A., and Zhang, F. (2013). Genome engineering using the CRISPR-Cas9 system. Nat. Protoc. *8*, 2281–2308. https://doi.org/10.1038/nprot.2013.143.

Romain, G., Senyukov, V., Rey-Villamizar, N., Merouane, A., Kelton, W., Liadi, I., Mahendra, A., Charab, W., Georgiou, G., Roysam, B., et al. (2014). Antibody Fc engineering improves frequency and promotes kinetic boosting of serial killing mediated by NK cells. Blood *124*, 3241–3249. https://doi.org/10.1182/blood-2014-04-569061.

Rotiroti, M.C., Buracchi, C., Arcangeli, S., Galimberti, S., Valsecchi, M.G., Perriello, V.M., Rasko, T., Alberti, G., Magnani, C.F., Cappuzzello, C., et al. (2020). Targeting CD33 in chemoresistant AML patient-derived xenografts by CAR-CIK cells modified with an improved SB transposon system. Mol. Ther. *28*, 1974–1986. https://doi.org/10.1016/j.ymthe.2020.05.021.

Schmid-Burgk, J.L., Honing, K., Ebert, T.S., and Hornung, V. (2016). CRISPaint allows modular base-specific gene tagging using a ligase-4-dependent mechanism. Nat. Commun. *7*, 12338. https://doi.org/10.1038/ncomms12338.

Somanchi, S.S., Senyukov, V.V., Denman, C.J., and Lee, D.A. (2011). Expansion, purification, and functional assessment of human peripheral blood NK cells. JoVE. https://doi.org/10.3791/2540.

Song, F., and Stieger, K. (2017). Optimizing the DNA donor template for homology-directed repair of double-strand breaks. Mol. Ther. Nucleic Acids *7*, 53–60. https://doi.org/10.1016/j.omtn.2017.02.006.

Suzuki, K., Tsunekawa, Y., Hernandez-Benitez, R., Wu, J., Zhu, J., Kim, E.J., Hatanaka, F., Yamamoto, M., Araoka, T., Li, Z., et al. (2016). In vivo genome editing via CRISPR/Cas9 mediated homology-independent targeted integration. Nature *540*, 144–149. https://doi.org/10.1038/nature20565.

Vallera, D.A., Felices, M., Mcelmurry, R., Mccullar, V., Zhou, X., Schmohl, J.U., Zhang, B., Lenvik, A.J., Panoskaltsis-Mortari, A., Verneris, M.R., et al. (2016). IL15 trispecific killer engagers (TriKE) make natural killer cells specific to CD33+ targets while also inducing persistence, in vivo expansion, and enhanced function. Clin. Cancer Res. *22*, 3440–3450. https://doi.org/10.1158/1078-0432.ccr-15-2710.

Wang, J., Declercq, J.J., Hayward, S.B., Li, P.W.L., Shivak, D.A., Gregory, P.D., Lee, G., and Holmes, M.C. (2016). Highly efficient homology-driven genome editing in human T cells by combining zinc-finger nuclease mRNA and AAV6 donor delivery. Nucleic Acids Res. *44*, e30. https://doi.org/10.1093/nar/gkv1121.

STAR★METHODS

KEY RESOURCES TABLE

REAGENT or RESOURCE	SOURCE	IDENTIFIER
Antibodies		
CD107a	BD Pharmingen™	Cat# 555801; RRID:AB_396135
CD33	MiltenyBiotech	Cat# 130-111-020; RRID:AB_2657559
Alexa Flour647-AffiniPure Goat Anti-Human IgG-Fcy	Jackson Immuno Research Labs	Cat# 109-605-098; RRID:AB_2337889
140Ce_cPARP	Fluidigm	N/A
151Eu_CD123	Fluidigm	N/A
153Eu_HLA-DR	Fluidigm	N/A
154Sm_CD69	Fluidigm	N/A
156Gd_CyclinB1	Fluidigm	N/A
165Ho_pRb	Fluidigm	N/A
175Lu_Perforin	Fluidigm	Cat# 3175004B, RRID:AB_2895147
142Ce_CD7	Fluidigm	N/A
148Nd_CD34	Fluidigm	Cat# 3148001B, RRID:AB_2810243
152Sm_CD33	Fluidigm	N/A
167Er_CD99	Fluidigm	N/A
139La_CD41	Fluidigm	N/A
143Nd_CD71	Fluidigm	N/A
144Nd_CD94	Fluidigm	N/A
149Sm_CD127	Fluidigm	Cat# 3149011, RRID:AB_2661792
155Gd_PD-1	Fluidigm	Cat# 3155009B, RRID:AB_2811087
158Gd_Ki67	Fluidigm	N/A
159Tb_CD38	Fluidigm	N/A
160Gd_CD14	Fluidigm	Cat# 3160006, RRID:AB_2661801
164Dy_CD15	Fluidigm	Cat# 3164001B, RRID:AB_2810970
166Er_NKG2D_CD314	Fluidigm	Cat# 3166016B, RRID:AB_2892110
168Er_CD13	Fluidigm	N/A
169Tm_NKG2A_CD159	Fluidigm	Cat# 3169013B, RRID:AB_2756426
170Er_pH2AX	Fluidigm	N/A
172Yb_CD10	Fluidigm	N/A
174Yb_CD20	Fluidigm	N/A
161Dy_CD16	Fluidigm	N/A
146Nd_CD8a	Fluidigm	Cat# 3146003B, RRID:AB_2687833
150Nd_CD117	Fluidigm	N/A
157Gd_CD45RA	Fluidigm	N/A
162Dy_CD11b	Fluidigm	N/A
163Dy_CD64	Fluidigm	N/A
171Yb_CD200	Fluidigm	N/A
173Yb_CD19	Fluidigm	N/A
176Yb_pCREB	Fluidigm	N/A
115In_CD45	Fluidigm	N/A
194Pt_H3K27me3	Fluidigm	N/A
147Pm_CD56	Fluidigm	N/A
113In_CD3	Fluidigm	N/A

(*Continued on next page*)

Continued

REAGENT or RESOURCE	SOURCE	IDENTIFIER
209Bi_pHH3	Fluidigm	N/A
89Y_CD235	Fluidigm	N/A
Bacterial and virus strains		
AAV6	Andelyn Biosciences	https://andelynbio.com
Biological samples		
Buffy coat	RedCross	N/A
Chemicals, peptides, and recombinant proteins		
Human recombinant IL-2 Protein	STEMCELL Technologies	Cat#15065
RosetteSep™ Human NK Cell Enrichment Cocktail	STEMCELL Technologies	Cat# 15065
Ficoll-Paque® PLUS	Cytiva	Cat# 17144003
AIM-V	Gibco	Cat# 12055083
CTS™ Immune Cell SR	Gibco	Cat# A2596101
IDTE pH 7.5 (1X TE Solution)	Integrated DNA Technologies, Inc.	Cat# 11-01-02-02
Alt-R® Cas9 Electroporation Enhancer, 10 nmol	Integrated DNA Technologies	Cat# 1075916
Alt-R® S.p. HiFi Cas9 Nuclease V3, 500 μg	Integrated DNA Technologies	Cat# 1081061
Recombinant Human Siglec-3/CD33 Fc Chimera Protein, CF (50ug)	R&D Systems	Cat# 1137-SL-050
Platinum™ Taq DNA polymerase high fidelity kit	Thermofisher	Cat# 11304011
Critical commercial assays		
CRISPRevolution sgRNA EZ Kit	Synthego, Menlo Park, CA	https://www.synthego.com/products/crispr-kits/synthetic-sgrna
Maxpar MCP9 Antibody Labeling Kit, 111Cd—4 Rxn	Fluidigm	Cat# 201111A
Maxpar® X8 Multimetal Labeling Kit—40 Rxn	Fluidigm	Cat# 201300
Bio-Plex Pro Human Cytokine 8-plex	Bio-Rad	Cat# M50000007A
xCELLigence RTCA Reagents, Kits & Accessories	Agilent Technologies	https://www.agilent.com
IMT assay (anti-CD29) tethering kit	Agilent Technologies	Cat# 8100008
Experimental models: Cell lines		
mbIL21-expressing feeder cells (FC21)	Lead contact	Available for academic institutions upon request
Kasumi-1	American Type Culture Collection (ATCC)	RRID:CVCL_0589
HL-60	American Type Culture Collection (ATCC)	RRID:CVCL_0002
Oligonucleotides		
Primers/oligonucleotides used in the study	Integrated DNA Technologies, Newark NJ	see Table S1
Recombinant DNA		
DNA encoding mCherry	GenScript	https://www.genscript.com
DNA encoding CARs	GenScript	https://www.genscript.com
Software and algorithms		
Flow Jo v10	TreeStar	https://www.flowjo.com
GraphPad Prism software version 8.2.1	GraphPad Software	https://www.graphpad.com
xIMT software	Agilent Technologies	https://www.agilent.com

RESOURCE AVAILABILITY

Lead contact

Further information and requests for resources and reagents should be directed to and will be fulfilled by the lead contact, Dean A. Lee (dean.lee@nationwidechildrens.org).

Materials availability

This study generated various mCherry and CAR encoding plasmids that can be shared by the lead contact upon request. FC21 cells for NK cell expansion can be shared by the lead contact upon request.

Data and code availability

- All data reported in this paper will be shared by the lead contact upon request.
- This paper does not report original code.
- Any additional information required to reanalyze the data reported in this paper is available from the lead contact upon request.

EXPERIMENTAL MODEL AND SUBJECT DETAILS

Cell lines and primary cultures

The irradiated mbIL21-expressing feeder cells (FC21) are genetically modified human female chronic myeloid leukemia cell line K562. Before irradiation, the cells were cultured and grown in RPMI 1640 medium containing 10% fetal bovine serum (FBS) and penicillin/streptomycin, and maintained at 37C, 5% CO2. Human acute myeloid leukemia cell lines HL-60 (CCL-240^{TM}) and Kasumi-1 (CRL-2724^{TM}) were purchased from American type culture collection (ATCC). Primary human AML cells (AML-10) were obtained from a pediatric patient with relapsed M5 AML and passaged in NOD-SCID mice. Human primary NK cells were isolated from buffy coats obtained from healthy donor and purchased from Red Cross. The buffy coats were exempt from IRB approval. The stimulated cells were cultured for 7 days in serum-free AIM-V/ICSR expansion medium containing 50 IU/mL of IL-2 (Moseman et al., 2020).

METHOD DETAILS

Human NK cell purification and expansion

NK cells were purified as previously described (Denman et al., 2012; Somanchi et al., 2011). Briefly, NK cells were isolated from PBMC collected from healthy individuals using RosetteSep^{TM} Human NK Cell Enrichment Cocktail. Purified NK cells were stimulated with irradiated feeder cells (FC21) comprised of K562 transduced with 4-1BBL and membrane-bound IL-21 (mbIL21) at a ratio of 2:1 (feeder:NK) as previously described (Denman et al., 2012; Somanchi et al., 2011).

ATAC-seq assay

Freshly-isolated (naive) and FC21-expanded NK cells from two donors were cryopreserved in aliquots of 100,000 viable cells/vial before processing for ATAC-seq. ATAC-seq was performed as previously described (Buenrostro et al., 2013). DNA libraries were sequenced using Illumina HiSeq 2500 at 50 bp paired-end reads.

Cas9/RNP electroporation for targeting AAVS1 in NK cells

AAVS1 was targeted using gRNA (crRNA: 5′GGGGCCACTAGGGACAGGAT) via electroporation of Cas9/RNP into NK cells seven days after stimulation with FC21 as described before (Naeimi Kararoudi et al., 2018). Briefly, 3×10^6 expanded NK cells were harvested and washed twice with 13 mL of PBS followed by centrifugation for 5 min at 400 g and aspiration of PBS. The cell pellet was resuspended in 20ul of P3 Primary Cell 4D-Nucleofector Solution. 5ul of pre-complexed Cas9/RNP (Alt-R® CRISPR-Cas9 crRNA, Alt-R® CRISPR-Cas9 tracrRNA, or preassembled synthetic sgRNA (Synthego, Menlo Park, CA) and Alt-R® S.p. HiFi Cas9 Nuclease V3) (Integrated DNA Technologies, Inc., Coralville, Iowa), targeting AAVS1 and 1ul of 100uM electroporation enhancer (Alt-R® Cas9 Electroporation Enhancer) were added to the cell suspension. The total volume of 26ul of CRISPR reaction was transferred into 4D-Nucleofector^{TM} 16-well Strip and electroporated using program EN-138. After electroporation, the cells were transferred into 2 mL of media containing 50 IU of IL-2 in a 12 well plate and incubated at 37 degrees and 5% CO_2 pressure. Two days post electroporation, cells were stimulated with 2×10^6 feeder cells, and 8 mL fresh media complemented with 50 IU was added in cell suspension and kept in a T25 flask.

Inference of CRISPR Edits (ICE) mutation detection assay

To measure the indel rate in AAVS1^{KO} NK cells, the Cas9/RNP targeted site was PCR amplified using forward and reverse primers described in Table S1. The amplicons were sequenced using Sanger sequencing, and results were analyzed using ICE (Hsiau et al., 2018) (Synthego, Menlo Park, CA).

RNA-seq sample preparation and sequencing

Total RNA was purified from NK cells after fresh isolation or after 14 days of expansion on FC21, using the Total RNA Purification Plus Kit (Norgen Biotek, ON, Canada). The resulting total RNA was sequenced and analyzed as described before (Foltz et al., 2018).

AAV6 production

The transgenes cloned into ssAAV or scAAV plasmids were packaged in AAV6 capsids as described before (Mendell et al., 2017). Figures 2A and 2B provide the detail of the constructs.

Combining Cas9/RNP and AAV6 to generate mCherry and CAR NK cells

A media change and resuspension at 5 × 10^5 cells per mL was performed on day 6 of NK cell expansion one day before experimental manipulation. The NK cells were electroporated with Cas9/RNP targeting AAVS1 on day 7, as described above. Thirty minutes after electroporation, 3 × 10^5 live cells were collected and resuspended at 1 × 10^6 cells per mL in media containing 50 IU IL2 (Novartis) in a 24 well plate in a total volume of 300ul. For each transduction condition with ssAAV6 or scAAV6 to deliver HDR or CRISPaint DNA encoding mCherry or CD33CARs, we transduced 3 × 10^5 electroporated cells with 300K MOI (10-500K MOI if needed). Negative controls included as NK cells that were not electroporated, or were electroporated with Cas9/RNP but not AAV transduced, or were transduced with 300K MOI of AAV6 without electroporation of Cas9/RNP. The day after electroporation and transduction, we added 300ul of fresh media containing 50 IU of IL2 to each well without changing the old media. The cells were kept in culture for 48 h after electroporation and were then re-stimulated with 2 × 10^6 feeder cells and kept in a total volume of 2 mL media containing 50 IU in 12 well plate, without changing the old media. 48 h later, 8 mL fresh media supplemented with IL2 was added to cells, a total volume of 10 mL was kept in a T25 flask. At day 7 post-transduction, cells were re-stimulated with feeder cells at a ratio of 1:1 and grown for one more week, every 2 days fresh media was added to the cells.

Flow cytometry for detection of CAR-NK cells and cancer cells

7 days and 14 days following electroporation, 5 × 10^5 NK cells were washed twice with staining buffer containing 2% FBS in PBS. Next, 2.5ug of recombinant human siglec-3/CD33 Fc chimera protein, (CF; R&D systems #1137-SL-050) was added to cell suspension in a total volume of 80ul and incubated for 30 min at 4C. Cells were washed twice with staining buffer before staining with 2ul of Alexa Fluor® 647 affinipure goat anti-human IgG, Fcγ fragment specific, (Jackson ImmunoResearch #109-605-098) at 1:100 ratio in 200ul of staining buffer and kept at 4C for 30 min. 5 × 10^5 AML cell lines were resuspended in 50ul of staining buffer for 30 min in the presence of 2ul of CD33 antibody. Once stained, cells were washed twice with staining buffer then acquired on MacsQuant flow cytometers. Flow cytometry data were analyzed using FlowJo software (FlowJo, LLC).

Cytotoxicity assay

Cytotoxicity assays were performed for 3-4 h as described previously using a calcein-acetoxymethyl-release assay (Somanchi et al., 2011; Lee et al., 2010). Cytotoxicity was assessed against Kasumi-1, HL60, or AML10 cells at different effector:target ratios as defined in Figures 6A–6E.

CD107a staining

NK cells and cancer cells were cocultured at 10:1 ratio and supplemented with 20ul of PE mouse anti-human CD107a antibody (BD Pharmingen™, #555801) in a total volume of 220ul in a 96 well plate at 37C incubator for 90 min. The cells were washed with staining buffer once and analyzed on MacsQuant flow cytometer.

Donor 1 – Day 9 post Sort
300K MOI – scPAMPAM
Donor 1 – Day 9 post Sort
500K MOI – ss800

Cytokine secretion assay

Expanded wildtype or expanded CD33-Gen2 CAR-NK cells from three donors were co-cultured with AML target cells (Kasumi-1) in 96 well plates at a ratio of 1:10. After 4 h, the supernatants were collected and quantified using a multi-plex cytokine assay according the manufacturer's instructions (Bio-Plex Pro Human Cytokine 8-plex Assay, #M50000007A, Bio-Rad) on the Bioplex 200 system.

PCR-based detection of transgenes integration

In-out PCR was performed using 2 pairs of primers (Figures 5A and 5B and Table S1) designed inside or outside of the CD33CAR constructs. We also added a set of primers to amplify 1200 bp right and left flanking region of Cas9 targeting and transgene integration site (Figure 5A). PCRs were performed using the Platinum™ Taq DNA polymerase high fidelity kit.

Targeted locus amplification (TLA)

For the whole-genome mapping of CD33CAR-Gen2 integration, we used the TLA technology (Cergentis B.V.) (de Vree et al., 2014). The genomic DNA from CD33CAR-expressing NK cells was isolated using Qiagene DNeasy Blood & Tissue Kit and crosslinked, fragmented, and re-ligated using the kit provided by Cergentis, then submitted to Cergentis for sequencing.

Real-time potency assessment for suspension target cells killed by WT and CD33CAR NK cells

The xCELLigence RTCA MP instrument (ACEA Biosciences) was utilized as previously described (Cerignoli et al., 2018). Briefly, the CD29 tethering reagent was coated on the plate (2 μg/mL, for 3 h at 37°C) to immobilize the Kasumi cell line, seeded at 6×10^4/well. After 20-24 h, WT or CD33CAR NK cells were added at indicated E:T ratios. An "effector cell only" control was included in the presence of tethering reagent. Cell Index values reflecting viable target cell adherence were applied to xIMT software to plot percentage cytolysis.

AML-NK cell Co-Culture

Cells were grown in SFEM II (StemCell, Cambridge, MA) supplemented with the following cytokines; SCF, IL-6, TPO, FLT3, GM-CSF, G-CSF, IL-3 (20 ng/mL) and EPO (10 ng/mL). A de-identified primary AML sample was obtained from OSU Leukemia Tissue Bank consistent with Declaration of Helsinki. NK or CAR-NK cells at a target:effector ratio of 1:2 were cultured for either 6 or 24 h. Following culture, cells were prepared for staining as previously described (Behbehani et al., 2012).

Mass cytometry staining and analysis

Fixed cells were washed with CSM as previously described (Rahman et al., 2016). Antibodies used for this study are listed in key resources table. Samples were resuspended in 1:20 dilution of four elemental equilibration beads (Fluidigm) at a concentration of 1 million cells/mL. FCS generated files were normalized using a normalization tool developed by Finck et al. and analyzed on Cytobank (www.cytobank.org) (Finck et al., 2013; Kotecha et al., 2010).

Once the singlet gate was established, cells were identified using markers and analyzed using SPADE (Qiu et al., 2011).

QUANTIFICATION AND STATISTICAL ANALYSIS

Data are presented as mean ± standard error of the mean (SEM). Statistical significance was determined GraphPad Prism software (9) using Student's *t* test, one-way or two-way ANOVA as indicated and where appropriate adjusted for multiple comparison. p values < 0.05 were considered statistically significant and indicated by * ($p < 0.05$), ** ($p < 0.01$), or *** ($p < 0.001$). The number of biological replicates including NK cell donors included in each experiment is indicated in the figure legend. Except for the CyTOF analysis, NK cells expressing mCherry, and flow cytometry on cancer cells, all experiments were performed as at least 2 independent experiments. The number of biological and technical replicates for each experiment are indicated in the figures and/or figure legends.